Plasma and trap-based techniques for science with antimatter

J. Fajans[1,a] and C. M. Surko[2,b]
[1] *Physics Department, University of California Berkeley*
[2] *Physics Department, University of California San Diego*

ABSTRACT

Positrons (i.e., antielectrons) find use in a wide variety of applications, and antiprotons are required for the formation and study of antihydrogen. Available sources of these antiparticles are relatively weak. To optimize their use, most applications require that the antiparticles be accumulated into carefully prepared plasmas. We present an overview of the techniques that have been developed to efficiently accumulate low energy antiparticles and create specially tailored antiparticle plasmas. Techniques are also described to create tailored antiparticle beams. Many of these techniques are based on methods first developed by the nonneutral plasma community using electron plasmas for increased data rate. They have enabled the creation and trapping of antihydrogen, they have been critical to studies of positron and positronium interactions with matter, including advanced techniques to characterize materials and material surfaces; and they have led to the creation and study of the positronium molecule. Rather than attempting to be comprehensive, we focus on techniques that have proven most useful, applications where there has been significant, recent progress, and areas that hold promise for future advances. Examples of the latter include ever more precise comparisons of the properties of antihydrogen and hydrogen, tests of gravity using antihydrogen and positronium atoms, and efforts to create and study phases of the many-electron, many-positron system.

I. INTRODUCTION

In the past few decades, the use of antimatter for scientific and technological purposes has become increasingly important. Positrons are used to characterize materials and material surfaces [1], and for positron emission tomography (PET) which is used in drug design and to study metabolic processes [2]. Scientific applications include tests of quantum electrodynamics (QED), creation of exotic species such as positronium (Ps) and the positronium molecule ($e^+e^-e^+e^-$, symbol Ps_2) [3, 4], and understanding fundamental positron interactions with ordinary matter including atoms and molecules [5, 6]. One of the newest developments is the ability to create high-quality beams of positronium atoms for precision measurements and for fundamental physics tests, such as the gravitational attraction of antimatter to our (matter) earth [7, 8].

Antiprotons play a central role in the formation and study of antihydrogen (the bound state of the antiproton and the positron and the simplest stable antiatom). Antihydrogen is being used to test the CPT theorem (i.e., the predicted invariance of relativistic quantum field theories under charge conjugation, parity inversion and time reversal) and the gravitational attraction of antimatter to matter. Results have been obtained for the 1S-2S transition [9], and the hyperfine transition [10], which, by an absolute energy metric [11], are some of the most precise tests to-date of the CPT theorem. Crude measurements of the interaction of antihydrogen with the earth's gravitational field have also been performed [12]. CPT tests such as a comparison of the proton/antiproton magnetic moment and mass have also been performed with isolated antiprotons [13, 14]. These tests have attracted much attention, both in the physics community and with the lay public.

Sources of antiparticles are relatively weak. Positrons can be obtained from a variety of radioisotopes, nuclear reactors, and linear electron accelerators (LINACS) [15]. However, while one can easily obtain many Coulombs of electrons at amp-strength currents, only *pico-Coulombs* at *sub-pico-amp currents* are available in the case of positrons. Antiprotons for low-energy research with antimatter are available only at the Antiproton Decelerator (AD) [16] at CERN in Geneva, Switzerland. Once degraded to below 5 kV, bunches of only ~ 10^5 antiprotons are delivered by the AD, at a rate of one bunch every two minutes. The new upgrade to the AD, ELENA [17], is expected to deliver 10–100 times more useable antiprotons.

Some applications demand tailored antiparticle beams. Depending on the application, one might want fine lateral focusing, high areal densities, low-energy beams, nearly monoenergetic beams, or short temporal pulses. Alternatively, one might want to deliver intense bursts of large numbers of antiparticles.

Other applications work best with confined antiparticles. Because antiparticles suffer annihilation when they come in contact with matter, they must be confined in vacuum, typically in an electromagnetic trap. The antiparticles form a charged cloud which is often in the plasma state. The focus of this article is to describe the techniques required to accumulate antiparticles and manipulate the resulting plasmas, tailored for specific applications. The techniques described here rely heavily on research in plasma and beam physics [15]. In particular, many useful processes are extensions of techniques developed to tailor more conventional single-component plasmas (i.e., plasmas composed of electrons or ions) and mixed-species nonneutral plasmas.

II. ANTIMATTER PLASMAS IN TRAPS

A. Penning-Malmberg traps

A wide variety of electromagnetic traps have been used to confine positrons, including Penning traps, magnetic mirrors and levitated magnetic dipoles [18-22]. For long-time confinement of large numbers of positrons or antiprotons, the method of choice is some

[a] joel@physics.berkeley.edu
[b] csurko@ucsd.edu

variant of the Penning-Malmberg (PM) trap [23]. As shown in Fig. 1, PM traps use a uniform magnetic field for radial confinement and an electrostatic potential well in the magnetic field direction for axial confinement. These traps are used to confine gases or plasmas whose constituents are all of the same charge sign, though in antihydrogen synthesis, two adjacent, oppositely charged plasmas are merged.[1] As pointed out by O'Neil, for a cold, magnetized plasma consisting of particles with a single sign of charge, the canonical angular momentum in a PM trap can be approximated as

$$L_z \approx \frac{eB}{2}\sum_j r_j^2, \qquad (1)$$

where z is the direction of the magnetic field B, and r_j is the radial position of particle j with charge e (SI units) [24]. If there are no torques on the plasma, the angular momentum is constant and the plasma cannot expand. Thus, confinement is nominally perfect, and the plasma can reach an equilibrium state [25].

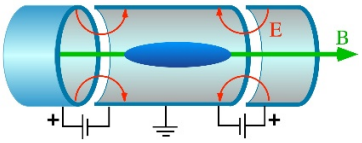

Fig. 1. Schematic diagram of a Penning-Malmberg trap for the confinement of plasmas consisting of particles of a single sign of charge, here biased for positive charges. Typical electrode radii and lengths are several centimeters. The "parallel" direction z is defined to be aligned with the trap and magnetic axes, and "perpendicular" refers to the orthogonal directions.

A plasma in a PM trap produces a strong radial electric field. This field results in an $\boldsymbol{E} \times \boldsymbol{B}$ drift in the azimuthal direction, which causes the plasma to spin about the magnetic axis. With good confinement, the shears in the plasma damp out, and the plasma rotates as a rigid rotor at frequency

$$f_E = \frac{en}{4\pi\varepsilon_0 B}, \qquad (2)$$

where n is the plasma density [26] and ε_0 is the permittivity of free space. Depending upon the application, PM traps can operate at a variety of magnetic fields (e.g., 0.01–7 tesla). As discussed in the next section, particle cooling is frequently necessary. At high (e.g., tesla-strength) magnetic fields, naturally occurring cyclotron radiation can fill this role, while at low B, other techniques, such as collisions with a molecular gas, are used.

Plasma expansion and losses in PM traps have been extensively investigated [15, 24, 27]. They are believed to be due to torques induced by azimuthal asymmetries. The transport induced by these torques cannot yet be predicted by theory for a particular device. Thus, when constructing a trap, one endeavors to minimize magnetic and electrostatic asymmetries. Even with a perfectly symmetric trap, patch potentials can produce deleterious asymmetries [28]. Recent evidence suggests that colloidal-graphite-coated electrodes are superior to electroplated gold in minimizing patch asymmetries [29].

In practice, plasma confinement times in PM traps range from milliseconds to hours and scale approximately as B^2 [27]. There is evidence that confinement is superior in multi-ring PM traps [30], which utilize many short electrodes extending over the length of the plasma, rather than one long electrode, as depicted in Fig. 1. These short electrodes can be used to generate a near-harmonic potential. Investigation of the possibly better performance of such multi-ring traps is a fruitful area for further research.

B. Ultra-long-time confinement

If long-time confinement is needed, antiparticles can be transferred to an ultra-high vacuum (UHV) PM trap where annihilation losses are minimized (cf. Fig. 2) [31]. Transfer efficiencies can be in excess of 90 %, but can also be lower depending upon the specific circumstances. Antimatter can be routinely confined in such traps for days, and in exceptional cases, years [13, 32], using traps mostly or entirely enclosed by surfaces at 4.2 K. Pressures below 10^{-14} Torr are readily obtained in such cryogenic traps, and can go as low as $\sim 10^{-18}$ Torr [13, 32]. When necessary, plasma expansion can be minimized or eliminated by applying rotating electric fields [i.e., the "rotating wall" (RW) technique [33]]. The RW technique and long confinement also require good particle cooling, which can be provided by cyclotron radiation in strong (e.g., tesla-strength) magnetic fields. We defer further discussion of the performance and limits of UHV traps to the later sections on cyclotron cooling and the RW technique.

C. Buffer-gas PM traps

Sources of positrons typically produce particles with energies of kilo-electron volts or higher. There is not yet an efficient way to trap particles at these energies, and so various materials ("moderators") are used to slow them to electron volt energies [1, 15, 34-36], whereupon they can be trapped in a buffer-gas trap (BGT). The BGT (cf. Fig. 2) is a modified PM trap that employs a stepped potential well in the B direction and corresponding regions (stages) of varying gas pressure. The highest-pressure region (stage I) is used to trap the particles by electronic excitation of a molecule (N_2 is the molecule of choice) in one transit through the trap. Subsequent collisions act to move the particles to stages of lower potential and gas pressure, where annihilation is slower (e.g., annihilation times ~ 100 s). Buffer-gas traps using solid Ne moderators can have as high as 30% trapping efficiency [34].

The operating cycle of the BGT will depend upon the application. For energy-resolved scattering and annihilation experiments, one desires to avoid space charge effects. Trap operation is typically a few Hz, with microsecond pulses of 10^3 – 10^4 positrons. In other applications, one may want large bursts of positrons in which case accumulation (and hence cycle) times can be of order 100 s.

[1] Usually, but not always, the charge clouds are in the plasma regime, which is defined by $\lambda_D < L$ and $n(\lambda_D)^3 > 1$, where $\lambda_D = (\varepsilon_0 T/ne^2)^{1/2}$ is the Debye length, ε_0 is the permittivity of free space, T is the plasma temperature, L is the characteristic dimension of the plasma, and n is the plasma density.

Discussed below are techniques developed to "bunch" the positron bursts into nanosecond pulses.

Even in the low-pressure regions of BGT traps annihilation can be problematic. When longer time confinement times are needed, the positrons can be transferred to an UHV trap such as those discussed above [31].

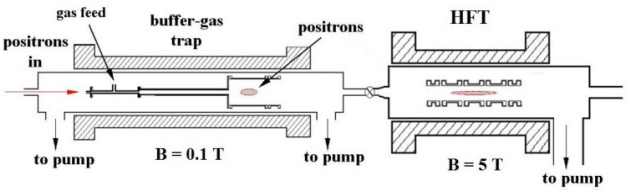

Fig. 2. Schematic diagram of a three-stage buffer-gas positron trap and an adjacent high-magnetic-field UHV trap (HFT) [31]. In the BGT, each of the latter two stages are at successively lower buffer-gas pressures and lower electrical potentials.

III. PLASMA DIAGNOSTICS

Diagnostics measuring the plasma density, radius, length, and temperature have played a key role in the development of the physics of antimatter plasmas. Experience has shown that the progress of underdiagnosed experiments has suffered. Many of these diagnostics were first developed by the nonneutral plasma community, but the unique conditions of antimatter experiments (sometimes tenuous plasmas, cryogenic traps with poor access, ultralow plasma temperatures) have made applying them difficult.

Total particle number. Because antimatter plasmas typically contain only one sign of charge, the total charge can be detected by destructively dumping the plasma onto a Faraday cup, or if the plasma is tenuous, a microchannel plate (MCP). Alternatively, the charge can be counted by detecting the annihilation byproducts (gamma rays for positrons, pions for antiprotons) on particle detectors (commonly scintillators or Si-based devices). Calibration of annihilation-based diagnostics is complicated by solid angle, scattering, and absorption issues.

Plasma density profile and aspect ratio. The areal plasma density (the density projected onto the transverse plane, typically in units of $[\mathrm{cm}^{-2}]$) can be determined by destructively dumping the plasma onto a phosphor screen and imaging the resultant light with a CCD camera. For a recent study of the difference in detection characteristics of phosphor screens for electrons and positrons, see Ref. [37]. Often, an MCP is used to brightness-enhance the image [38, 39]. Typically, the type of particle being detected is known beforehand. If not, there are other ways to distinguish them. For example, antiprotons are approximately a factor of 100 brighter than leptons on an MCP, and antiparticles will have characteristic annihilation products that can be detected separately.

The plasma aspect ratio (length to radius), and radial density profile $n(r)$ $[\mathrm{cm}^{-3}]$ can be determined numerically from the areal density, the total charge, and the confinement geometry [40]. The plasma profile and aspect ratio can also be determined by measuring the plasma axial bounce and breathing mode frequencies [41, 42]. While often useful, the reconstruction of the plasma parameters is hindered by wall effects, and, for needle-like (high aspect ratio) plasmas, by a numeric instability in the formulas for the mode frequencies.

Temperature. The parallel plasma temperature can be measured by lowering the barrier that confines the plasma slowly compared to the bounce time of the plasma particles. The most energetic plasma particles will escape first and can be counted with a Faraday cup or scintillators. The temperature can then be determined from the count *vs*. confinement voltage profile [43]. Only particles escaping from within a few Debye lengths of the plasma center contain temperature information. This makes the diagnostic difficult to operate at low temperatures (sub 100K), and an MCP is often necessary to amplify the signal from these few escaping particles. The temperature can be measured from just one plasma sample. To-date, this method of measuring the temperature has been most generally useful in antihydrogen trapping. However, there are other methods of measuring the temperature, several of which are described below. Of these, the modes diagnostics has been the most useful.

The perpendicular plasma temperature can be measured by using a magnetic gradient field to convert perpendicular to parallel energy in conjunction with an electrostatic energy barrier [44, 45]. This technique has the advantage that it measures the bulk distribution, rather than the Maxwellian tail distribution as is measured by the parallel temperature diagnostic described immediately above. However, the technique requires a gradient-producing coil as well as multiple plasma samples, and the samples must be nearly identical. To our knowledge, the technique has not been implemented for antimatter plasmas.

Plasma temperatures can also be measured by systematic trends in the bounce and breathing mode frequencies [46-48]. While this diagnostic has the advantage that it is nondestructive, it should be emphasized that this is a relative temperature diagnostic and does not yield absolute temperatures. Moreover, the numeric instabilities and wall effects previously mentioned hinder its applicability.

For a single component plasma, one can also extract small pulses of charge by lowering an end gate (i.e., as with the velocity measurement described in the previous paragraph). The charge, which will come from the region near the axis, has a Gaussian radial distribution with a $1/e$ width of two Debye lengths [49]. If other measures of the density are available, the width of the pulse provides a measurement of the plasma temperature.

Finally, the temperature can be determined by measuring the thermal fluctuations in the naturally excited plasma-mode amplitudes [50]. Unfortunately, this otherwise advantageous technique requires a true thermal equilibrium (i.e., without extrinsic noise) and good signal-to-noise. Consequently, it is difficult to apply at low temperatures (< 300K) or in a noisy environment.

IV. PLASMA MANIPULATION TECHNIQUES

A. Plasma cooling and temperature control

For most applications, good particle cooling is either desirable or necessary to avoid deleterious effects (e.g., ionization and/or positronium formation on background gas, and evaporative particle loss). Cooling methods include using a buffer gas and cyclotron radiation, as well as sympathetic cooling via laser-cooled ions and adiabatic and evaporative cooling.

Buffer gas cooling. Cooling of positrons using a molecular gas is now a well-established technique [15, 51, 52], and it is central to the operation of the buffer-gas positron trap. Where possible (initial trapping in a BGT being an exception), one tries to avoid energy loss by electronic excitation, since this occurs close in energy to positronium-atom formation which is a virulent positron-annihilation loss process. Thus, one relies on molecular collisions and the associated excitation of vibrations and rotations for cooling (i.e., below the threshold for positronium atom formation). As long as the positrons do not form positron-molecule bound states (which are absent for many small molecules), annihilation (a key limitation of this technique) is relatively benign. Depending upon the choice of molecule, cooling times from energies of ~ 1 eV to 25 meV (11,600 to 300 K) range from < 10 ms to 1 s at gas pressures ~ 10^{-6} torr [52].

Molecular nitrogen N_2 is used in BGT for the initial trapping (energy loss ~ 10 eV/collision), since the cross section for electronic excitation near the threshold is large at energies before positronium formation dominates. The N_2 is frequently augmented by CF_4 or SF_6 for more rapid vibrational cooling to lower temperatures. The rates for cooling to 300 K due to vibrational and rotational collisions are compared for three molecules in Fig. 3 [52]. At 10^{-6} Torr of these gases, positron annihilation times are ~ 10^2 s. A recently developed cryogenic BGT operating at 50 K used the CO molecule [29], which has a permanent dipole moment and hence enhanced rotational energy loss. The CO has a sufficiently high vapor pressure so as to not freeze out at 50 K. Buffer gas cooling to temperatures as low as 20 K appears to be possible with H_2, but cooling will be slow (i.e., comparable to N_2).

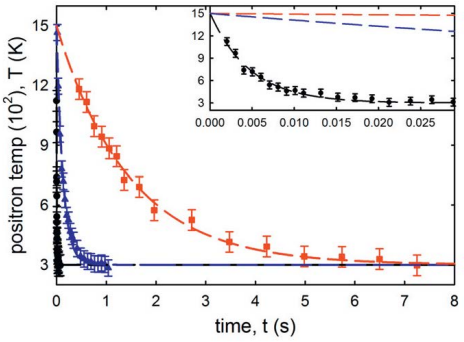

Fig. 3. Positron cooling on molecular vibrations and rotations for (●) CF_4, (▲) CO, and (■) N_2 gases at 300 K (horizontal line) [52]. The data are normalized to 1 μtorr and shifted to coincide at t = 0 s; the dashed lines show an exponential fit for each case. Inset shows CF_4 in more detail. The corresponding cooling times to 1/e are 4.8, 130, and 1,500 ms/μtorr for CF_4, CO, and N_2.

Cyclotron cooling. In a magnetic field, the cyclotron orbits of the particles result in the emission of radiation. This can be an efficient cooling mechanism for the perpendicular degrees of freedom of electrons and positrons [53, 54]. Except under extreme conditions of high fields and low temperatures [55], collisions thermalize the parallel and perpendicular energies at a rate much faster than the cooling itself. Including this thermalization, the free-space cooling rate (in units of s^{-1}) is

$$\Gamma_c = \frac{1}{T}\frac{dT}{dt} = \frac{2e^2\,\Omega_c^2}{9\pi\varepsilon_0 mc^3} \approx 0.26\left(\frac{B}{1T}\right)^2, \qquad (3)$$

where T is the plasma temperature, $\Omega_c = eB/m$ is the cyclotron frequency, m is the particle mass, and c is the speed of light. Cyclotron cooling has been exploited extensively at tesla-strength magnetic fields. While generally not as fast as buffer-gas cooling, it is compatible with UHV vacuum environments and thus avoids the use of a buffer gas and the associated annihilation loss.

Recently, a resonant cavity was used to enhance the cyclotron cooling rate (cf. Figs. 4 and 5) [56]. As in the Purcell effect, the cavity enhances the cyclotron rate [57]. Electron plasmas have been cooled to 10 K with a rate 100 times faster than the spontaneous rate given by Eq. (3). Fast cooling has been observed in fields as low as 0.15T, where the free-space cyclotron cooling rate is very small. While there is some limitation on the number of particles that can be cooled in this manner, resonant cavity cooling offers considerable potential, particularly when one wants to operate in UHV conditions and/or at low magnetic fields.

Sympathetic cooling on electrons. A key advance in antimatter physics was the development of techniques to trap and cool energetic antiprotons. Antiprotons from CERN's LEAR (and later the AD) facility can be slowed by a degrader. About 0.5% of the antiprotons in the 5.3 MeV AD beam can be slowed to below 5 keV. These antiprotons can then be "barn-door trapped" with an efficiency approaching 100% by the application of a fast-rising electrode potential, resulting in a cloud of 0 – 5keV antiprotons in a PM trap [58]. The antiprotons can then be cooled to ~5 meV temperatures by collisions with cyclotron-cooled electrons [59]. Note that because of baryon number conservation, antiprotons do not annihilate on electrons.

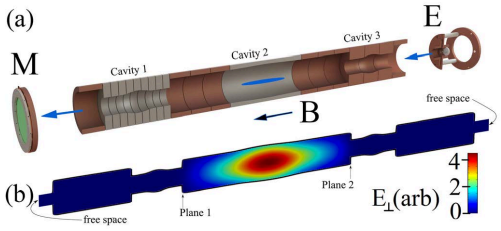

Fig. 4. (a) Electrodes of a PM trap designed to exploit resonant-cavity cyclotron cooling in resonant Cavity 2. Cavities 1 and 3 act as waveguides beyond cutoff. (b) the simulated electric field intensity for the TE_{111} mode in Cavity 2 [56].

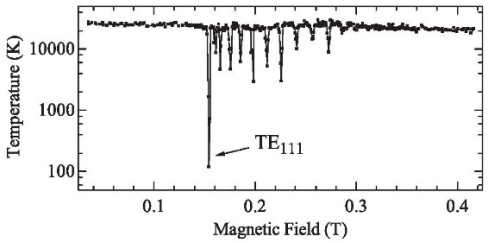

Fig. 5. Measured temperatures of electron plasmas initially at 26,000 K and cooled for 8 s at the indicated magnetic field values using the apparatus in Fig. 4. The dips occur upon excitation of TE_{11X} modes [56].

Sympathetic cooling using laser-cooled ions. Small numbers of positrons (~ 1000) have been sympathetically cooled to $T < 5$ K when they were co-loaded in a PM trap with a larger number (~10^5) of laser-cooled Be^+ ions. However, deleterious centrifugal separation was observed [60]. Further work is necessary to determine the extent to which centrifugal separation is an intrinsic limitation, and also to determine if a large number of positrons ($\geq 10^6$) can be cooled with a smaller number of ions (e.g., ~ 10^5) [61].

Adiabatic expansion. Adiabatic expansion can be used to cool nonneutral plasmas [45] to temperatures below 10K. In this process, the electrostatic confining potential well is expanded axially. By conservation of the bounce adiabatic invariant, the plasma will cool. For best results, the well must be expanded slowly compared to the particle bounce time, since this preserves the adiabatic nature of the expansion. While the plasma only directly cools in the axial direction, Coulomb collisions thermalize the plasma in all directions.

Evaporative cooling. Nonneutral plasmas can also be cooled by evaporative cooling, in which the electrostatic confining well barrier is lowered so that the hottest plasma particles escape. The remaining plasma then re-thermalizes on the collision time scale. An example of the use of this method to cool antiprotons is shown in Fig. 6.

Both adiabatic expansion and evaporative cooling have proven useful and important in antimatter physics experiments (e.g., see Refs. [62-64] for cooling both positrons and antiprotons. Expansion cooling retains all of the particles, which is advantageous. It does, however, expand the plasma axially, which lowers the plasma density. Evaporative cooling necessarily involves loss of particles, though with care, this loss can be minimized. Further, angular momentum conservation requires that the plasma expand radially [24], which also lowers the plasma density.

B. Plasma density control—the "rotating wall technique"

If there are no torques on a plasma in a PM trap, angular momentum is conserved and there is no net expansion. However, realistic plasma traps always have asymmetries which act to expand the plasma. If one injects angular momentum by deliberately applying a torque, one can compress the plasma as required by Eq. (1) and counteract the intrinsic expansion. Such torques can be applied by the "rotating wall" (RW) technique illustrated in Fig. 7. It has been used to compress single-component plasmas, charged gases in the single particle regime, and cold, high density ion crystals [33, 65-70]. To use this technique, phased electrical signals at some frequency f_{RW} are used to drive azimuthally segmented sectors of an electrode surrounding an axial portion of the plasma. The electric field induces a dipole moment, resulting in a torque. This torque increases the rotation frequency of the plasma and thus acts to increase the density as per Eq. (2) (see Fig. 8). The RW technique can be used to increase the plasma density and/or to achieve long term particle confinement (e.g., days, weeks or longer). It has proven useful in both BG and UHV traps [15, 69, 70].

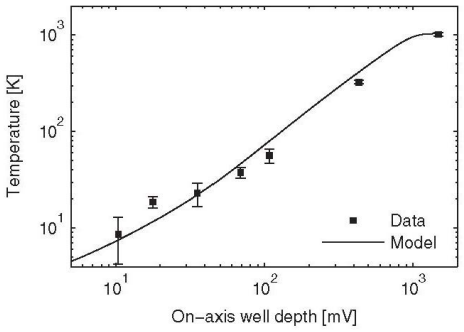

FIG. 6. (a) Six steps of evaporative cooling of antiprotons, resulting in a temperature decrease from 1,000 K to 9 K (■). The temperature *vs.* the on-axis well depth is compared with a model calculation (solid line). The initial number of antiprotons was approximately 45,000 at an on-axis well depth of 1.5 eV. Approximately 6 % of the particles remain at the final temperature of 9 K. See Ref. [63] for details.

The torque due to the RW fields does work on the plasma and hence produces heating [33]. Thus, RW compression requires a plasma cooling mechanism. This cooling can be provided by the background gas in BG traps, by cyclotron cooling in UHV traps, or laser cooling using co-loaded ions. For antiprotons, sympathetic cooling on co-trapped cyclotron-cooled electrons can be used [71]. One group, however, has reported RW compression without an obvious cooling mechanism [72].

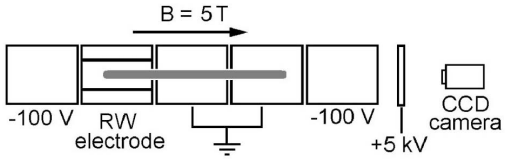

Fig. 7. Apparatus for RW compression of single component, negatively charged plasmas. The areal density profile is measured by accelerating the particles onto a phosphor screen and measuring the resulting light, as discussed in Section III.

Particle heating is reduced when the asymmetry-induced transport is minimized, and this is desirable. For a single component plasma in a PM trap with good confinement, the plasma density *n* approaches a constant, independent of the radial position in the plasma. As illustrated in Fig. 9, when the applied frequency $f_{RW} > f_E$, the plasma can be made to spin up until the

two frequencies are approximately equal, namely $f_E \approx f_{RW}$ (the so-called "strong drive regime" of RW compression) [33, 73]. Experience has shown, however, that PM traps with relatively good confinement are required in order to be able to operate in this strong drive regime.

The Brillouin density limit, $n_B = B^2/(2\mu_0 mc^2)$, where μ_0 is the permeability of free space, is the maximum plasma density that can be confined in a magnetic field B [74]. As shown in Fig. 9, for plasmas in PM traps using buffer gas cooling, densities of 17% of n_B have been achieved. That this is not 100 % of n_B can likely be understood as limited by molecular collisions in the relatively strong radial electric fields near n_B [75]. In contrast, while higher absolute densities have been achieved in cyclotron-cooled plasmas in high-field UHV traps, the fraction of the Brillouin limit achieved is much smaller (e.g., $n/n_B \leq 10^{-3}$). The relatively poor performance in this regime is not understood and is a subject of ongoing research.

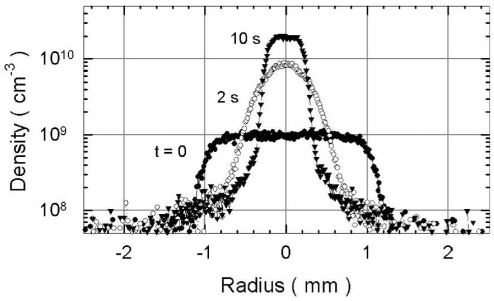

Fig. 8. Rotating wall compression of an electron plasma starting at time $t = 0$ [76]. Note the log density scale. The constant density profiles at t = 0 and 10 s are characteristic of rigid-rotor rotational motion [i.e., as described by Eq. (2)].

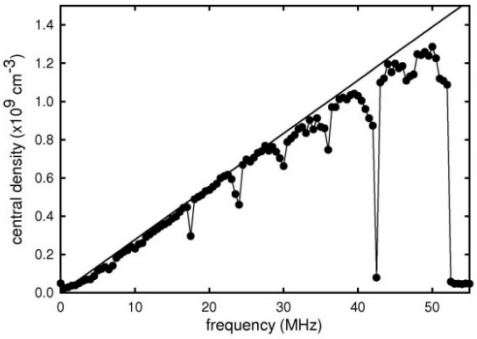

Fig. 9. Change in density of a positron plasma as a function of applied RW frequency when a constant frequency is applied [15]. The solid line corresponds to $f_E = f_{RW}$, characteristic of the strong drive regime. For this experiment, B = 0.04 T, and the maximum density achieved is 17% of the Brillouin density limit. The sharp drops in density at specific frequencies are due to static asymmetries that couple to low-order plasma modes and act as a drag on the plasma.

C. Combined techniques to provide unprecedented plasma reproducibility

The parameters of plasmas loaded into PM traps can vary substantially from loading to loading. Some of this variation comes from the particle source itself: for positron sources, for instance, due to the variations in pumping, the quality and age of the moderator, and other factors. In some experiments, the number of trapped positrons can easily vary by a factor of two. Other variations can come from the transport of particles from low to high magnetic field, where magnetic mirroring can play a significant role. Mirroring can be reduced by transferring the particles at an axial energy much greater than the plasma temperature; however, as discussed below, this can introduce other problems.

In some applications, such as the trapping of antihydrogen, the reproducibility of the plasma loading is critical. Reproducibility can be dramatically improved by simultaneously employing strong-drive RW fields (SDR) (which sets the plasma density) and evaporative cooling (EVC) (which sets the plasma on-axis potential). So long as the temperature is low, setting the density and the on-axis potential fully specifies the remaining plasma parameters, including the plasma radius and total charge. An example of this procedure, called SDREVC [62], is shown in Fig. 10. The stability engendered by SDREVC has led to more than an order of magnitude increase in the formation rate of trappable antihydrogen.

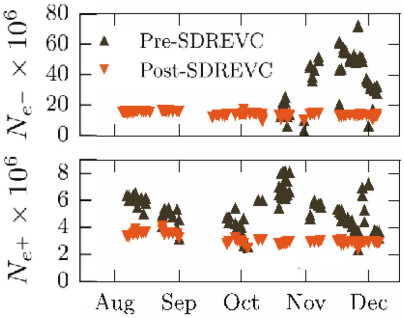

Fig. 10. Stability of the electron and positron plasmas (the former for sympathetic cooling of the antiprotons) used to create antihydrogen atoms before and after plasma tailoring by radial compression and evaporative cooling (SDREVC) [62].

D. Plasma purity control for antihydrogen formation

While some plasma processes used to form antihydrogen require or tolerate multispecies plasmas, many require that the plasmas be pure. Some techniques to purify the plasmas are given below.

Removal of cooling electrons. Antiprotons are initially captured from the AD by sympathetic cooling on electrons. These electrons must be removed from the mixed antiproton/electron plasma before the antiprotons can be moved substantial distances (e.g., to another trap). Once moved, the antiprotons are frequently remixed with new electrons to re-cool them. These electrons must be subsequently removed before the antiprotons are further processed to make antihydrogen. The electrons are usually removed by momentarily lowering the electrostatic confinement well trapping the mixed plasmas. Because the electrons are much lighter than the antiprotons, they will escape the trap before the antiprotons respond significantly. This process, sometimes called "e-kicking," is somewhat delicate. Lowering the barrier too much

or for too long a time, heats or even loses the antiprotons, while lowering the barrier too little or for too short a time, does not remove all the electrons.

To obtain pure, cold, antiprotons plasmas, it is often necessary to perform several cycles of ever deeper, albeit incompletely effective e-kicks. Between each cycle, the antiprotons are sympathetically re-cooled on the ever-diminishing number of electrons. E-kicking also expands the remaining plasma, counteracting sympathetically cooled antiproton compression. Thus, it is frequently necessary to do compression in several stages, separated by the partial e-kicks. Consequently, the optimal tuning of this process is subtle [77], but when well-tuned, few antiprotons are lost.

Positron cleaning. When positrons or other particles are transported long distances and/or into higher field regions, they are often transported at axial energies well above the initial plasma temperature. For example, a 50 eV transport energy is often used. This energy is greater than the ionization and positronium formation thresholds for background neutrals, and so the particles can become contaminated with background ions. This is particularly troublesome for positrons, because the background ions are typically positively charged, and are hence confined by the same electrostatic well as used to confine the positrons. These ions can cause fast expansion and plasma heating, and so they need to be removed before the positrons are further processed. This can be accomplished by a modified e-kicking process, in which the ejected, now pure, positrons are then re-caught in a potential well downstream, or by driving the ions out of the positron plasma with a frequency resonant with the ion bounce frequency. When done carefully, few positrons are lost by these cleaning operations.

E. Autoresonance.

Under certain circumstances, a nonlinear oscillator can be made to phase lock to a drive signal if the drive frequency is slowly swept through the linear (low amplitude) resonant frequency of the system [78]. This phenomenon, called autoresonance, has proven useful to *coherently* manipulate plasmas in PM traps. An example is shown in Fig. 11 where the longitudinal motion of an antiproton cloud in a PM trap has been excited and the cloud released at various mean energies set by the end-gate potential [79]. In another application, development of a practical multicell positron trap for large numbers of positrons [80, 81], an electron plasma was moved across the magnetic field by autoresonant excitation of the diocotron mode (i.e., the bulk rotation of the plasma around the trap axis caused by the plasmas interaction with its image) [74].

The combination of trapping and plasma manipulation techniques has established the ability to create a wide variety of trapped antimatter plasmas. Table I gives some examples.

Table I. Examples of operating parameters for antimatter plasmas in PM traps, the plasma length and radius, L_p and r_p, temperature and density, T and n, space charge potential, V_s, and the confinement time τ_c. **Positrons:** in gas-cooled traps: UCSD – three-stage BGT, UCR – 2-stage BGT, FPSI – First Point Scientific BGT and accumulator; and in cyclotron- cooled traps: the ALPHA [82], ATHENA [83] and ATRAP [84] collaborations at CERN. **Antiprotons:** the ALPHA [82], ATRAP [64], and AEgIS [77] collaborations at CERN.

Device	B (T)	L_p (cm)	r_p (mm)	T (eV)	n 10^8 (cm)$^{-3}$	N_{max} 10^7	V_s (V)	τ_c (s)
Positrons								
UCSD	0.1	10	6	0.03	0.02	30	15	300
UCR	0.09	1	0.5	0.03	1	0.1	0.01	1
FPSI	0.04	10	0.5	0.05	12	10	~10	~1000
ALPHA†	1	1	0.7	0.001	1	3	0.2	
ATHENA†	3				26	120		~9000
ATRAP	1					400	530*	~14400
Antiprotons								
ALPHA†	1	1	1	0.0006	0.01	0.005	0.02	
ATRAP	3.7			0.0003		0.3		
AEgIS	4.46		0.17		0.2	0.007		

† Not achieved simultaneously *Confinement voltage

V. TRAP-BASED ANTIPARTICLE BEAMS

Different applications require different types of optimization of antiparticles beams generated from PM-trapped antiparticle plasmas. Described here are some frequently used techniques.

A. Narrow energy spreads

Buffer-gas trap-based positron beams with narrow energy spreads have proven useful for studying positron scattering and annihilation processes [5, 6]. A simple method to create a beam is to trap and cool positrons in a PM trap and then carefully raise the bottom of the confining potential well to force them over an end gate barrier. Typically, the plasma is allowed to cool to the ambient gas temperature T_g, in which case the achievable spread in total energy is approximately (3/2) $k_B T_g$. In more detail, the beam energy distribution can be described by an exponentially modified Gaussian (EMG) distribution [85]. The energy distribution in the motion perpendicular to B is Maxwellian, but the parallel energy depends on the dynamics of the expulsion of the particles from the PM trap and the shape of the confining potential well. Energy spreads of 40 meV FWHM have been achieved using a 300 K buffer gas and 7 meV with a gas at 50 K [15, 29].

B. Short temporal pulses

For applications such as study of high-density gases of positronium atoms, one would like short temporal bursts of antiparticles. Examples include the creation of dense gases of positronium atoms at material surfaces [86], matching lasers to collections of Ps atoms for precision spectroscopy, and preparing long-lifetime, high-Rydberg-state Ps atoms for advanced Ps beams [8]. For example, the more focused in space and time the positron burst, the more efficiently it can be matched to laser pulses for the manipulation of atoms (e.g., high-Rydberg Ps). Temporal bunching technology is very highly developed due to its importance in tailoring electron beams, and so techniques are readily available for positron applications at the level of a few hundred picoseconds. One would like to achieve such short pulse durations for applications such as single-shot positron lifetime spectroscopy [87].

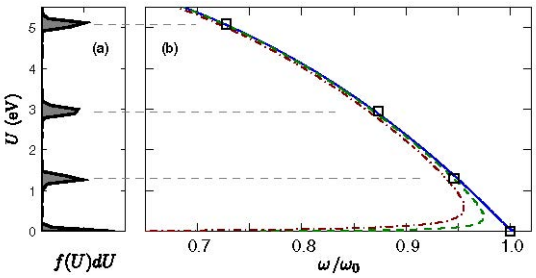

Fig. 11. Autoresonant release of a cloud of antiprotons from a potential well. The frequency is swept downward from the linear value for this well with bounce frequency $\omega_0/2\pi = 410$ kHz. The open squares (right) denote the mean beam energy U of each distribution $f(U)$ (left), plotted against the final drive frequency (dashed lines). See Ref. [79] for details.

One technique for temporal pulse compression is to confine the plasma in a PM trap inside a stack of short cylindrical electrodes. Shown in Fig. 12 are data using such a harmonic "buncher" to time-compress a pulse of positrons from a BGT accumulator. In this technique, a positron plasma is confined in a multi-ring PM trap, the potential is quickly ramped up to a parabolic profile, with the minimum in the potential some distance downstream, thus producing a time focus at that location. Alternately, one can produce short temporal pulses from an accelerator-based source [88].

C. Beams with small transverse extent

The RW technique can be used to increase plasma density. This, in conjunction with carefully extracting positrons from the center of the plasma (i.e., center-line extraction), can produce magnetically guided beams with small transverse spatial extent (the limit being four Debye lengths) [49]. Such beams would aid in the use in positron microscopy to study material surfaces, as discussed further in the next section.

D. Electrostatic beams from trapped plasmas

Techniques have been developed to extract positron beams from the magnetic field of a PM trap into a field free region. This is difficult to do while simultaneously preserving beam quality. Techniques used to help maintain beam quality include transmission through a small hole in a high-permeability plate and use of a specially designed grid made of a similar material [89, 90]. If the objective is a beam with small transverse extent, this can be preceded by center-line extraction. Following extraction from the field, one can then focus the resulting particles electrostatically (frequently using a remoderator [91]). This latter process can be repeated to further focus the beam, albeit with some particle loss. Such narrow beams are of use, for example, in applications such as positron microscopy.

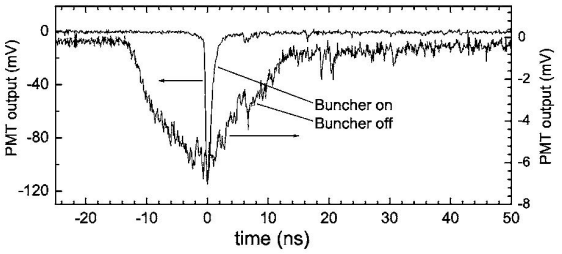

Fig. 12. Positron pulses with and without a harmonic buncher, showing time compression of a factor of approximately ten to < 2 ns [92].

E. Spin-polarized positron beams

For applications such as the creation and study of dense gases of Ps atoms, one would like to prepare the longer-lived spin S = 1 atoms. This has been done exploiting the fact that ^{22}Na positron sources emit spin-polarized positrons (i.e., since the positrons are produced *via* the weak interactions). The approximately 30% expected polarization was produced, and maintained even when the fast positrons from ^{22}Na were moderated in energy using solid neon and trapped in a BGT, followed by density increase using a RW and time-compressed using a harmonic buncher [93].

F. Trap-based positronium atom beams

High quality Ps beams are important for characterizing materials as well as for tests of fundamental physics such as the gravitational attraction of matter and antimatter. This is an area which has seen considerable progress recently, and one that holds much promise for the future.

High-Rydberg-state Ps beams. The positronium atom is unstable to electron-positron annihilation. The lifetime depends upon the spin of the atom and the principle quantum number of the state. The lowest order annihilation process for ground-state Ps atoms with S = 1 is decay by the emission of three gamma rays with a lifetime of 140 ns, while the S = 0 state decays by the emission of two gamma rays with a lifetime of 120 ps [94]. These short lifetimes pose an important constraint on the creation and utility of Ps beams.

One recent approach, offering considerable promise to produce high quality Ps beams, exploits trap-based beam technology to

produce focused, time-compressed bursts of positrons. When incident upon a specially chosen material surface, bursts of Ps atoms are produced that can then be matched to laser pulses to produce high-Rydberg-state Ps atoms [95]. In these atoms, the overlap of the positron and electron wave functions is relatively small, resulting in much longer lifetimes (e.g., lifetime ≥ 100 μs for the n = 31 state).

If these Rydberg atoms are made in a strong electric field (so-called Stark states) [8], they can have large permanent dipole moments. They can then be manipulated (guided, focused) by suitably arranged regions of varying electric field. The schematic diagram of a recent experiment is shown in Fig. 13. Typical Ps energies are a few tenths of an eV. Potentially, this technique is an alternative method to form antihydrogen (ie., by the process of charge exchange of Rydberg Ps atoms with antiprotons) [96, 97] and long-lived, high quality Ps beams for antimatter gravity studies [8].

Higher-energy Ps beams using the Ps^- ion. A technique to form high-quality Ps beams at higher energies is illustrated in Fig. 14 [98]. It uses time-compressed pulses of positrons incident upon a Na-coated W foil to create the Ps^- ion (i.e., a positron and two electrons). The Ps^- is then accelerated and the excess electron laser stripped. This technique has produced Ps beams with energies from 300 eV to 3 keV and beam divergences of 0.3°. Alternately, it has been proposed to use a traveling optical lattice [99]. Among other applications, such beams offer considerable promise in studying material surfaces.

VI. APPLICATIONS ENABLED BY TRAPS AND TRAP-BASED BEAMS

We review here recent progress in key antimatter applications enabled by the plasma and trap-based tools discussed above and describe the potential impact of tools currently under development.

A. Formation, trapping and study of antihydrogen

As mentioned above, an exciting area of science with antimatter is the creation of antihydrogen atoms and precision tests of their properties compared with those of hydrogen. These activities are the focus of work by several world-wide collaborations at CERN's AD facility. Antihydrogen trap depths are less than 1 K. Consequently, antihydrogen experiments must be done with particles at very low particle energies. Plasma manipulation and beam formation techniques have played a critical role in maximizing the efficiency of antihydrogen formation and trapping. Important procedures include efficient antiparticle trapping, density and temperature control, and tailored mixing of positrons and antiprotons. (see Refs. [62, 100-102]). A recent success of this strategy is the newly developed SDREVC technique (cf. Sec. IV. C and Fig. 10) to prepare reproducible single-component positron and electron plasmas (the latter for sympathetic antiproton cooling) [62].

As a result of these and other advances, in the last decade antihydrogen trapping rates have increased from 0.1 to 300/h [103]. Figure 15 shows a precision measurement of the 1S – 2S energy transition in antihydrogen [9]. Another recent achievement is the single-photon excitation of the 1S – 2P (Lyman α) transition in antihydrogen [104]. This sets the stage for laser cooling the antiatoms and further increases in the precision of comparisons of the properties of antihydrogen and hydrogen. To-date, these comparisons have found no differences between the two. A current goal is to study the 1S – 2S transition with a precision comparable to that of hydrogen, which will require an increase in precision of approximately 10^3s.

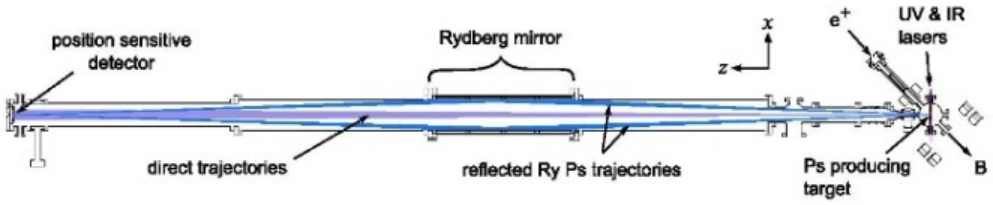

Fig. 13. Transmission and focusing of a high-Rydberg-state Ps beam [105]. Stark Ps states are formed using a UV and an IR laser. They are reflected from a specially prepared "Rydberg mirror" consisting of closely spaced rods approximately parallel to the beamline with alternating DC potentials that create a localized electric field near the surface. The mirror has a slight curvature such that low-field seeking Ps states are focused on a detector 6 m from the Ps source. See Ref. [105] for further details.

B. Cyclotron resonance magnetometry

Many of the experiments that can be done with antimatter require precise knowledge of the local magnetic field. For example, in experiments intended to measure gravity with antihydrogen atoms, a magnetic gradient of ~1.8 mT/m will produce a force on the antiatom equal to the force of gravity. Thus, a 1% accuracy free-fall experiment over a range of 0.3 m in a 1 T background field must control the field strength to the 10 ppm level.

Because antimatter traps are frequently in a UHV, cryogenic environment and have poor access, conventional magnetometry techniques employing NMR or Hall effect sensors are often infeasible. In this case, one is led to consider electron cyclotron resonance (ECR) magnetometry [106]. This technique uses variable-frequency microwaves to heat a plasma. From the frequency that maximizes the heating, as determined by the post-illumination plasma temperature, one can calculate the local

magnetic field assuming the frequency is the plasma cyclotron frequency [107].

Recently, two advances have led to ECR measurements at the 1 ppm level [108]. The first advance is the development of a technique to rapidly generate small electron plasmas. An extension of work to generate positron pulses [109], pulses from a reservoir of electron plasma are recaptured to form a succession of ECR target plasmas. These small target plasmas are required to measure the local field in the presence of magnetic gradients. Rapidly generated target plasmas are required to quickly complete a frequency scan, since the target plasma temperature is measured destructively (Sec. IV. A). The second advance is a methodology to reliably identify the cyclotron-frequency-resonance peak in the presence of many other heating resonances. This is accomplished by searching for the peak that does not move when the plasma electron bounce frequency is scanned. Research on this potentially important technique is ongoing.

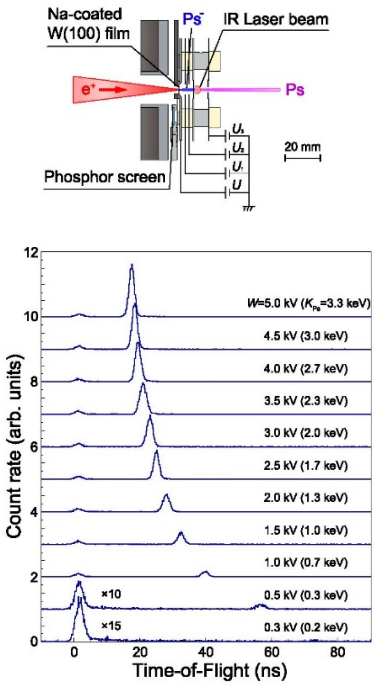

Fig. 14. Formation of a variable-energy Ps beam using Ps^- ions [98]. (above) Schematic diagram of the apparatus. A pulsed positron beam from a BGT is focused on a Na coated W film, which emits Ps^- ions. The ions are accelerated through an imposed potential drop V and then laser stripped to form the Ps beam. (below) Time-of-flight energy spectra of the resulting beam upon varying V from 0.3 to 3.5 kV.

C. Positron and positronium interactions with atoms, molecules and atomic clusters

The method described in Sec. V to produce pulsed, magnetically guided beams with narrow energy spreads has been exploited extensively for both positron scattering and annihilation studies [5]. It has enabled state-resolved measurements of the positron-impact cross sections for electronic excitation in atoms and molecules and vibrational excitation of molecules [5]. It has also led to the discovery and study of vibrational Feshbach resonances in positron annihilation in molecules, discovery and study of positron-molecule bound states, and measurement of positron-molecule binding energies for a wide variety of molecules [6].[2] Another interesting area for study is positron-induced fragmentation, which depends critically on the incident positron energy [110, 111]. The fact that positrons with energies close to the threshold for Ps formation produce little or no fragmentation has potentially important practical consequences [112]. The quest for colder beams to improve the energy resolution of such measurements is ongoing. At the current level of energy resolution (< 10 meV), maintaining this energy resolution downstream of the trap has proven to be challenging. This must be addressed.

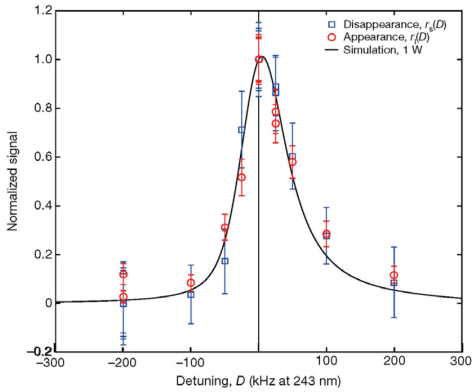

Fig. 15. A measurement of the antihydrogen two-photon 1S–2S transition is shown here corresponding to a relative precision of 2 x 10^{-12} [9]. The points show the number atoms that are detected (appearance) when "kicked" out of the system after illumination by light at various detuning frequencies, and the number of atoms that are missing (disappearance) after illumination as inferred by subtracting the number remaining after illumination from the number before illumination (done with multiple, repeated ensembles.) The line is the result of a simulation with 1W of laser power.

Electrostatic (as opposed to magnetically guided) beams have advantages, particularly in measuring angularly resolved scattering cross sections. Techniques exist to tailor positron pulses and then extract them from the magnetic field to create electrostatic beams that can be used for this purpose, however they have yet to be fully exploited.

Study of positron interactions with clusters has been discussed as a fruitful area for investigation [6] (e.g., positronic "cage states" in C_{60} clusters [113]). Qualitatively, clusters should behave as large molecules. Thus, they should exhibit resonant attachment and bound states, greatly enhancing annihilation rates and providing information about the target. Positron-induced Auger emission could give information about cluster surfaces [114]. However, thus

[2] While it is predicted that positrons bind to many atoms, the lack of low-lying excitations in atoms has, to date, hindered study of this process.

far, there have been no experiments with clusters, and so this is an interesting area for future investigation.

Positronium atoms couple differently to matter than do electrons or positrons, and so they give unique information [115]. The new generation of positronium beams can potentially shed light on Ps interactions with atoms and molecules, which is a subject of current interest [116].

D. Positron studies in condensed matter and materials physics

Trap-based beams offer many advantages for research in this area, but also have yet to be fully exploited [117, 118]. In the case of positrons, advantages include the possibility of single-shot positron-annihilation-lifetime spectroscopy (PALS) [87], pulsed beams for enhanced signal to noise in positron-induced Auger electron spectroscopy, and rotating-wall radial plasma compression and centerline beam extraction for spatial focusing (e.g., a positron microscope). While useful with all types of positron sources, this might be particularly beneficial at a high-flux reactor or LINAC-based positron beam facility [114].

The new generation of positronium beams offers many important avenues for future investigation of condensed matter phenomena. This arises from the fact that the Ps atom is qualitatively different (i.e., light, uncharged) probe particle, as compared with electrons, positrons or neutral atoms (e.g., He atom diffraction). The use of metal-organic framework (MOF) materials to create nearly monochromatic Ps beams [119], and the technique to create high-Rydberg-state atoms, offer complementary tools with which to conduct a variety of surface analysis experiments. A longstanding goal in this area is to study surfaces using Ps-atom diffraction [120]. The Ps beam described in Ref. [98] is an important step toward this goal. Another goal is to test the quantum reflection of Ps atoms from solid surfaces [121].

E. Bose-condensed gases of positronium atoms (Ps BEC)

Shown in Fig. 16 is a schematic view of the phase diagram for the many-electron, many-positron system. One fascinating possibility is to create a Ps-atom BEC. Bose condensation requires high densities of cold Ps atoms, which can potentially be achieved by implanting several-keV, partially spin-polarized positrons from a ^{22}Na source into a material with a cavity below the surface [122]. The positrons will cool, pick up electrons to become Ps atoms and diffuse into the cavity. After the two-gamma decays, the remaining atoms will be in long-lived S =1 states. If they are sufficiently cold and dense, they will transition to the BEC state [3]. The light mass of the Ps atoms lowers the requirements on n and T to achieve the BEC relative to that for ordinary neutral atoms. For example, for a Ps density of 10^{19} cm^{-3}, the transition temperature is T_c= 90 K.

Experiments are in progress to achieve such a state. They employ a BGT and accumulator with a RW, buncher and pulsed magnetic field to create bursts of ~ 10^8 positrons, which will then be extracted from the magnetic field and electrostatically metal remoderator to further increase beam emittance ($\epsilon \equiv D\sqrt{\Delta E_\perp/E_0}$, where E_0 is the beam energy and D the diameter, and $\Delta E_\perp$ is the spread in transverse energies). It is planned that the beam would then be accelerated and refocused on a suitable material to form a dense Ps focused on a gas and a Ps BEC [3].

F. Electron-positron plasmas

Another many-body electron-positron state, shown in Fig. 16, is the classical "pair" plasma, where the Debye length is small compared to the dimensions of the charge cloud and $n\lambda_D^3 > 1$, where λ_D is the Debye length. Such a plasma has long been predicted to have distinctly different properties than conventional electron-ion plasmas [123] but has yet to be studied in the laboratory. It has been proposed to confine such a plasma in variety of traps, including a stellarator, levitated magnetic dipole, magnetic mirror and a Penning-Paul trap [20-22, 124, 125]. Research on creating a pair plasma is currently underway. As part of this effort, preliminary experiments using a permanent magnet to mimic a dipole field have demonstrated the efficient loading of small numbers of positrons using **E** x **B** plates [126] and single-particle positron orbits with lifetimes > 1 s [127].

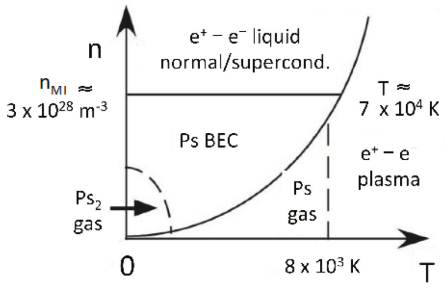

Fig. 16. Schematic (only) phase diagram of the electron-positron system as a function of density n and temperature T. The density n_{MI} of the metal-insulator transition is indicated. While this quantum phase is beyond current technology, Ps_2 has been created and studied, and near-term studies of a Ps BEC and a classical pair plasma are possible. (Adapted from Ref. [128].)

A key impediment to creating a pair plasma is the difficulty in accumulating sufficiently large numbers of positrons (e.g., 10^{10} – 10^{12}), to be injected in a burst to enter the plasma regime. The confinement of such large numbers of particles in a conventional PM trap results in large space charge potentials and hence requires large confinement voltages. An alternative positron accumulation scheme, the so-called multicell trap, has been proposed to circumvent this impediment [81].

VII. KEY TOPICS FOR FUTURE RESEARCH

Much progress has been made in trapping antimatter, tailoring the resulting plasma, and then tailoring delivery with specific applications in mind. The successes, and in some cases, the lack of progress raises new opportunities and necessities for further research. Here we give some examples.

Improved plasma compression. The rotating wall technique has proven to be a key tool in working with both positrons and antiprotons. As discussed in Sec. IV. B, this technique can be used to approach within a factor of six or less of the Brillouin (the

maximum possible) density limit when operated at 0.04 T and using buffer-gas cooling. At higher magnetic fields, while the absolute density reached is somewhat larger, it is nowhere near the Brillouin limit, particularly at tesla-strength fields where one relies on cyclotron cooling. This limiting behavior is not currently understood. Given the importance of large antiparticle densities for many applications, this should be a priority for further investigation.

Colder positron gases and plasmas. Techniques to prepare clouds of colder positrons could be very useful. This might be accomplished using the resonant cavity cooling technique described above. Sympathetic cooling with laser-cooled ions might be another useful approach.

Improved positron/antiproton mixing. The techniques to mix positron and antiproton plasmas to create antihydrogen are poorly understood and are thus tuned empirically. Simulations which properly model the process might be informative. These simulations will need to model both the antiproton and positron dynamics, include radial spatial effects as well as all three momentum dimensions and properly model collisions. Ideally, the simulations would model the exact procedures used in the various experiments, including the details of antiproton injection and any simultaneous adiabatic expansion/evaporative/sympathetic cooling. They would be particularly useful if they were able to provide insights into improving the antihydrogen formation and trapping fraction [129-132].

Sympathetic cooling of positively charged antihydrogen atoms. The GBAR collaboration intends to prepare the atoms for an antihydrogen fountain using an intermediate step of sympathetically-cooled, positively-charged antihydrogen ions [133]. These anti-ions are the antimatter analog of negatively charged hydrogen ions. Both the generation and sympathetic cooling of these anti-ions will require further research.

Antihydrogen beams. The antihydrogen physics results to date have been obtained with trapped antiatoms. There are potential physics advantages to working with antihydrogen beams; primarily the transport of the antihydrogen out of the strong magnet field environment necessary for the synthesis of antihydrogen. Weak beams, not yet necessarily in the required ground state, have been created by the ASACUSA collaboration for hyperfine studies [134], and the AEGIS collaboration is attempting to make beams for gravity studies [135].

Handling more antiprotons and the creation of antideuterium. With the coming operation of CERN's ELENA ring, orders of magnitude more antiprotons are expected to be available [17]. Efficiently utilizing the additional antiprotons presents new challenges to mixing schemes. Conversely, with the capability of producing antideuterons at Brookhaven National Laboratory comes the possibility, albeit very challenging, of creating antideuterium [136]. Since vastly fewer antideuterons than antiprotons would be available, new positron/antideuteron mixing schemes with far more efficient utilization of the antideuterons will need to be developed.

Improved electron cyclotron resonance magnetometry. While ECR magnetometry has been perfected to the 1 ppm level, it is not yet clear that it will be useable in the strong magnetic field gradients in the ALPHAg antihydrogen experiment [137], especially as the ALPHAg magnets are ramped, which is an intrinsic part of the ALPHAg scheme. Moreover, the current ECR schemes only measures the on-axis field. The extension of this technique to the measurement of off-axis fields would be very useful.

Higher quality positronium-atom beams. Much progress has been made in creating high quality Ps beams, and ones with long-lived high-Rydberg-state atoms. That said, the particle fluxes achieved to date are quite small. This area is in its infancy, and one can likely expect future improvements in technique.

Spin polarized positrons. Spin polarized positrons would be useful in a number of applications. This raises the question as to whether techniques can be developed to spin-polarize trapped positrons from an unpolarized source such as the NEPOMUC beam at the Technical University of Munich [138] or increase the degree of polarization of positrons from a radioisotope source such as ^{22}Na. One possibility is to put a PM trap in a magnetic field gradient and extract positrons from one end. Unfortunately, one would need plasmas colder than 1 K to do this, which is at present very challenging.

Larger numbers of positrons. Creation of a pair plasma is an application where large numbers of positrons are required (e.g., $N \sim 10^{10}$ - 10^{12}). The practical capacity of a single PM trap is made difficult by space charge. The larger the number of particles confined, the larger the space charge potential and hence the larger the required confining potential. One could work with a single plasma with a very large confining potential, but it is thought that the large space charge may well result in electrical breakdown and/or unacceptable levels of expansion heating. As an alternative, the possibility of using a multicell trap with an array of PM traps arranged in parallel in a common vacuum and magnetic field is being pursued [81].

Portable antimatter traps. A portable trap with capacity $N \sim 10^{12}$ would be of interest for a variety of positron applications. For example, such a trap would useful at a location (a synchrotron or chip assembly line) where a separate positron source is undesirable. Such a trap is, in principal, possible (e.g., using a multicell trap). However, present superconductor magnets require low temperatures, and this is a key impediment. Thus, such a trap appears to hinge on the further development in magnet technology (i.e., high-T_c superconductors).

In parallel with work on the positron transport, the PUMA project at CERN [139] intends to capture and transport, by truck, 10^9 antiprotons from CERN's AD to their ISOLDE facility [140]. At ISOLDE, interactions between the antiprotons and exotic nuclei will be investigated. The BASE collaboration is considering transporting ~ 100 antiprotons out of the AD hall to a quieter environment to facilitate their measurements [141].

VIII. CONCLUDING REMARKS

Science with antimatter at low energies (e.g., tens of electron volts or less) is a relatively new area of investigation but one in which there has been much progress and one that offers considerable potential for future science and technology. This article focuses on the ways in which plasma techniques have played a central role in this research and a glimpse as to what the future might hold for further progress.

The capabilities to trap and cool positrons and antiprotons has increased dramatically since the first efforts in the 1980s. Numerous new techniques have been developed to create ever more dense and cold antiparticle gases and plasmas and to manipulate them in novel ways. Similarly, techniques have been developed for antiparticle delivery, frequently as specially tailored beams. Of particular note is the recent success in matching clouds of antiparticles to laser radiation for further manipulation, and/or precision experiments.

These techniques have provided qualitatively new scientific insights and technological capabilities. The trapping and cooling of antiprotons, positrons and electrons enabled the first successful formation of low-energy antihydrogen atoms, and improvements in the plasma techniques have led to an increase in the antihydrogen trapping rate by more than a factor of 1000 in the last decade. These techniques also led to similar progress in understanding and exploiting positron-matter interactions. Examples include the creation and study of the positronium molecule (di-positronium, Ps_2), positron binding to molecules and atoms, and high-quality beams of positronium atoms.

The future of progress in this area is exceedingly bright. This is in no small part because of increased understanding of the importance of plasma techniques in the atomic physics, fundamental physics, and condensed matter physics communities, and the increased appreciation in the plasma community of problems and opportunities in these areas.

ACKNOWLEDGEMENTS

We wish to acknowledge helpful conversations with W. Bertsche, D. Cassidy, M. Charlton, J. Danielson, R. Greaves, A. Mills, Y. Nagashima, and D. van der Werf and a careful reading of the manuscript by F. Anderegg, W. Bertsche, M. Charlton, E. Gilson, J. Danielson and K. Zukor. This work has been supported by the U. S. DOE grants DE0016532, DE-SC0019271, and DE-SC0019346, and NSF grants PHY1702230 and PHY1806305.

REFERENCES

[1] P. J. Schultz and K. G. Lynn, Interaction of Positrons Beams with Surfaces, Thin Films, and Interfaces, Rev. Mod. Phys. **60**, 701 (1988).

[2] R. L. Wahl, Principles and Practice of Positron Emission Tomography, in *Principles and Practice of Positron Emission Tomography* (Lippincott, Williams and Wilkins, Philadelphia, PA, 2002).

[3] A. P. Mills, Possible Experiments with High Density Positronium, AIP Conf. Proc. **2182**, 030001 (2019).

[4] D. B. Cassidy, T. H. Hisakado, H. W. K. Tom, and A. P. J. Mills, Optical Spectroscopy of Molecular Positronium, Phys. Rev. Lett. **108**, 133402 (2012).

[5] C. M. Surko, G. F. Gribakin, and S. J. Buckman, Low-Energy Positron Interactions with Atoms and Molecules, J. Phys. B: At. Mol. Opt. Phys. **38**, R57 (2005).

[6] G. F. Gribakin, J. A. Young, and C. M. Surko, Positron-Molecule Interactions: Resonant Attachment, Annihilation, and Bound States, Rev. Mod. Phys. **82**, 2557 (2010).

[7] A. P. Mills and M. Leventhal, Can We Measure the Gravitational Free Fall of Cold {R}Ydberg State Positronium?, Nuc. Instrum. Meth. B **192**, 102 (2002).

[8] D. B. Cassidy, Experimental Progress in Positronium Laser Physics, Euro. Phys. J. D **72**, 53 (2018).

[9] M. Ahmadi, et al., Characterization of the 1s-2s Transition in Antihydrogen, Nature Letters **557**, 71 (2018).

[10] M. Ahmadi, et al., Observation of the Hyperfine Spectrum of Antihydrogen, Nature **548**, 66 (2017).

[11] M. Pospelov, Breaking of CPT and Lorentz Symmetries, Hyperfine Int. **172**, 63 (2006).

[12] C. Amole, et al., Description and First Application of a New Technique to Measure the Gravitational Mass of Antihydrogen, Nature Communications **4**, 1785 (2013).

[13] G. Gabrielse, et al., Thousandfold Improvement in the Measured Antiproton Mass, Phys. Rev. Lett. **65**, 1317 (1990).

[14] C. Smorra, et al., A Parts-Per-Billion Measurement of the Antiproton Magnetic Moment, Nature Letters **550**, 371 (2017).

[15] J. R. Danielson, D. H. E. Dubin, R. G. Greaves, and C. M. Surko, Plasma and Trap-Based Techniques for Science with Positrons, Rev. Mod. Phys. **87**, 247 (2015).

[16] S. Maury, The Antiproton Decelerator: Ad, Hyperfine Inter. **109**, 43 (1997).

[17] W. Bartmann, et al., The Elena Facility, Phil. Trans. Royal Soc. A **376**, 20170266 (2018).

[18] C. M. Surko, A. Passner, M. Leventhal, and F. J. Wysocki, Bound States of Positrons and Large Molecules, Phys. Rev. Lett. **61**, 1831 (1988).

[19] C. M. Surko, M. Leventhal, and A. Passner, Positron Plasma in the Laboratory, Phys. Rev. Lett. **62**, 901 (1989).

[20] H. Boehmer, M. Adams, and N. Rynn, Positron Trapping in a Magnetic Mirror Configuration, Phys. Plasmas **2**, 4369 (1995).

[21] H. Higaki, et al., Simultaneous Confinement of Low-Energy Electrons and Positrons in a Compact Magnetic Mirror Trap, N. J. Phys. **19**, 023016 (2017).

[22] H. Saitoh, et al., Stable Confinement of Electron Plasma and Intital Results on Positron Injection in Rt-1, in *Non-Neutral Plasma Physics Viii* (AIP Conference Proceedings, Melville, NY, 2013), Vol. 1521, p. 63.

[23] J. H. Malmberg and J. S. DeGrassie, Properties of Nonneutral Plasma, Phys. Rev. Lett. **35**, 577 (1975).

[24] T. M. O'Neil, A Confinement Theorem for Nonneutral Plasmas, Phys. of Fluids **23**, 2216 (1980).

[25] C. F. Driscoll, J. H. Malmberg, and K. S. Fine, Observation of Transport to Thermal Equilibrium in Pure Electron Plasmas, Physical Review Letters **60**, 1290 (1988).

[26] D. H. E. Dubin and T. M. O'Neil, Trapped Nonneutral Plasmas, Liquids, and Crystals (the Thermal Equilibrium States), Rev. Mod. Phys. **71**, 87 (1999).

[27] C. F. Driscoll and J. H. Malmberg, Length-Dependent Containment of a Pure Electron-Plasma Column, Phys. Rev. Lett. **50**, 167 (1983).

[28] A. Christensen, private communication (2019).

[29] M. R. Natisin, J. R. Danielson, and C. M. Surko, A Cryogenically Cooled, Ultra-High-Energy-Resolution, Trap-Based Positron Beam, Appl. Phys. Lett. **108**, 024102 (2016).

[30] T. Mohamed, A. Mohri, and Y. Yamazaki, Comparison of Non-Neutral Electron Plasma Confinement in Harmonic and Rectangular Potentials in a Very Dense Regime, Phys. Plasmas **20**, 012502 (2013).

[31] C. M. Surko, R. G. Greaves, and M. Charlton, Stored Positrons for Antihydrogen Production, Hyperfine Interactions **109**, 181 (1997).

[32] S. Sellner, et al., Improved Limit on the Directly Measured Antiproton Lifetime, New J. Phys. **19**, 083023 (2017).

[33] J. R. Danielson and C. M. Surko, Radial Compression and Torque-Balanced Steady States of Single-Component Plasmas in Penning-Malmberg Traps, Phys. Plasmas **13**, 055706 (2006).

[34] R. G. Greaves and C. M. Surko, Solid Neon Moderator for Positron Trapping Experiments, Can. J. Phys. **51**, 445 (1996).

[35] A. P. Mills and E. M. Gullikson, Solid Neon Moderator for Producing Slow Positrons, Appl. Phys. Lett. **49**, 1121 (1986).

[36] A. P. Mills, Further Improvements in the Efficiency of Low-Energy Positron Moderators, Appl. Phys. Lett. **37**, 667 (1980).

[37] E. V. Stenson, U. Hergenhahn, M. R. Stoneking, and T. S. Pedersen, Positron-Indeuced Luminescence, Phys. Rev. Lett. **120**, 147401 (2018).

[38] G. B. Andresen, et al., Antiproton, Positron, and Electron Imaging with a Microchannel Plate/Phosphor Detector, Rev. Sci. Instrum. **80**, 123701 (2009).

[39] A. J. Peurrung and J. Fajans, A Pulsed Microchannel-Plate-Based Non-Neutral Plasma Imaging System, Rev. Sci. Instrum. **64**, 52 (1993).

[40] R. L. Spencer, S. N. Rasband, and R. R. Vanfleet, Numerical-Calculation of Axisymmetrical Nonneutral Plasma Equilibria, Phys. Fluids B **5**, 4267 (1993).

[41] D. H. E. Dubin, Theory of Electrostatic Fluid Modes in a Cold Spheroidal Non-Neutral Plasma, Phys. Rev. Lett. **66**, 2076 (1991).

[42] M. D. Tinkle, R. G. Greaves, and C. M. Surko, Low-Order Longitudinal Modes of Single-Component Plasmas, Phys. of Plasmas **2**, 2880 (1995).

[43] D. L. Eggleston, C. F. Driscoll, B. R. Beck, A. W. Hyatt, and J. H. Malmberg, Parallel Energy Analyzer for Pure Electron Plasma Devices, Phys. Fluids B **4**, 3432 (1992).

[44] T. Hsu and J. L. Hirshfield, Electrostatic Energy Analyzer Using a Nonuniform Axial Magnetic Field, Rev. Sci. Instrum. **47**, 236 (1976).

[45] A. W. Hyatt, C. F. Driscoll, and J. H. Malmberg, Measurement of the Anisotropic Temperature Relaxation Rate in a Pure Electron Plasma, Phys. Rev. Lett. **59**, 2975 (1987).

[46] M. D. Tinkle, R. G. Greaves, C. M. Surko, R. L. Spencer, and G. W. Mason, Low-Order Modes as Diagnostics of Spheroidal Non-Neutral Plasmas, Phys. Rev. Lett. **72**, 352 (1994).

[47] M. Amoretti, et al., Positron Plasma Diagnostics and Temperature Control for Antihydrogen Production, Phys. Rev. Lett. **91**, 055001 (2003).

[48] M. Amoretti, et al., Complete Nondestructive Diagnostic of Nonneutral Plasmas Based on the Detection of Electrostatic Modes, Phys. Plasmas **10**, 3056 (2003).

[49] T. R. Weber, J. R. Danielson, and C. M. Surko, Creation of Finely Focused Particle Beams from Single-Component Plasmas, Phys. Plasmas **13**, 123502 (2008).

[50] N. Shiga, F. Anderegg, D. H. E. Dubin, C. F. Driscoll, and R. W. Gould, Thermally Excited Fluctuations as a Pure Electron Plasma Temperature Diagnostic Phys. Plasmas **13**, 022109 (2006).

[51] T. J. Murphy and C. M. Surko, Positron Trapping in an Electrostatic Well by Inelastic Collisions with Nitrogen Molecules, Phys. Rev. A **46**, 5696 (1992).

[52] M. R. Natisin, J. R. Danielson, and C. M. Surko, Positron Cooling by Vibrational and Rotational Excitation of Molecular Gases, J. Phys. B **47**, 225209 (2014).

[53] T. M. O'Neil, Cooling of a Pure Electron Plasma by Cyclotron Radiation, Phys. Fluids **23**, 725 (1980).

[54] J. H. Malmberg, et al., Experiments with Pure Electron Plasmas, in *Non-Neutral Plasma Physics*, edited by C. W. Roberson and C. F. Driscoll (American Institute of Physics, New York, 1988), p. 28.

[55] M. E. Glinsky, T. M. O. Neil, M. N. Rosenbluth, K. Tsuruta, and S. Ichimaru, Collisional Equipartition Rate for a Magnetized Pure Electron Plasma, Physics of Fluids B **4**, 1156 (1992).

[56] E. D. Hunter, et al., Low Magnetic Field Cooling of Lepton Plasmas Via Cyclotron-Cavity Resonance, Phys. Plasmas **25**, 011602 (2018).

[57] E. M. Purcell, Spontaneous Emission Probabilities at Radio Frequencies, Proc. Am. Phys. Soc. **69**, 681 (1946).

[58] G. Gabrielse, et al., First Capture of Antiprotons in a Penning Trap: A Kiloelectronvolt Source, Phys. Rev. Lett. **57**, 2504 (1986).

[59] G. Gabrielse, et al., Cooling and Slowing of Trapped Antiprotons Below 100 MeV, Phys. Rev. Lett. **63**, 1360 (1989).

[60] B. M. Jelenkovic, A. S. Newbury, J. J. Bollinger, W. M. Itano, and T. B. Mitchell, Sympathetically Cooled and Compressed Positron Plasma, Phys. Rev. A **67**, 063406 (2003).

[61] N. Madsen, S. Jonsell, and F. Robicheaux, Antihydrogen Trapping Assisted by Sympathetically Cooled Positrons, New J. Phys. **16**, 063046 (2014).

[62] M. Ahmadi, et al., Enhanced Control and Reproducibility of Non-Neutral Plasmas, Phys. Rev. Lett. **120**, 025001 (2018).

[63] G. B. Andresen, et al., Evaporative Cooling of Antiprotons to Cryogenic Temperatures, Phys. Rev. Lett. **105**, 013003 (2010).

[64] G. Gabrielse, et al., Adiabatic Cooling of Antiprotons, Phys. Rev. Lett. **106**, 073002 (2011).

[65] X. P. Huang, et al., Precise Control of the Global Rotation of Strongly Coupled Ion Plasmas in a Penning Trap, Phys. Plasmas **5**, 1656 (1998).

[66] F. Anderegg, E. M. Hollmann, and C. F. Driscoll, Rotating Field Confinement of Pure Electron Plasmas Using Trivelpiece-Gould Modes, Phys. Rev. Lett. **81**, 4875 (1998).

[67] X. P. Huang, F. Anderegg, E. M. Hollmann, C. F. Driscoll, and T. M. O'Neil, Steady State Confinement of Nonneutral Plasma by Rotating Electric Fields, Phys. Rev. Lett. **78**, 875 (1997).

[68] R. G. Greaves and C. M. Surko, Radial Compression and Inward Transport of Positron Plasmas Using a Rotating Electric Field, Phys. Plasmas **8**, 1879 (2001).

[69] R. G. Greaves and J. M. Moxom, Compression of Trapped Positrons in a Single Particle Regime by a Rotating Electric Field, Phys. Plasmas **15**, 072304 (2008).

[70] C. A. Isaac, C. J. Baker, T. Mortensen, D. P. v. d. Werf, and M. Charlton, Compression of Positron Clouds in the Independent Particle Regime Phys. Rev. Lett. **107**, 033201 (2011).

[71] G. B. Andresen, et al., Compression of Antiproton Clouds for Antihydrogen Trapping Phys. Rev. Lett. **100**, 203401 (2008).

[72] N. Kuroda, et al., Radial Compression of an Antiproton Cloud for Production of Intense Antiproton Beams, Phys. Rev. Lett. **100**, 203402 (2008).

[73] J. R. Danielson, C. M. Surko, and T. M. O'Neil, High-Density Fixed Point for Radially Compressed Single-Component Plasmas, Phys. Rev. Lett. **99**, 135005 (2007).

[74] R. C. Davidson, Physics of Nonneutral Plasmas, in *Physics of Nonneutral Plasmas* (Addison-Wesley, Reading, MA, 1990).

[75] C. M. Surko, J. R. Danielson, and T. R. Weber, Accumulation, Storage and Manipulation of Large Numbers of Positrons in Traps II: Selected Topics, in *Physics with Trapped Charged Particles*, edited by M. Kroop, N. Madsen and R. C. Thompson (Imperial College Press, London, U. K., 2014), p. 129.

[76] J. R. Danielson and C. M. Surko, Torque-Balanced High-Density Steady States of Single Component Plasmas, Phys. Rev. Lett. **94**, 035001 (2005).

[77] S. Aghion, et al., Compression of a Mixed Antiproton and Electron Non-Neutral Plasma to High Densities, Euro. Phys. J. D **72**, 76 (2018).

[78] J. Fajans and L. Friedland, Autoresonant (Non Stationary) Excitation of a Pendulum, Plutinos, Plasmas and Other Nonlinear Oscillators, Am. J. Phys. **69**, 1096 (2001).

[79] G. B. Andresen, et al., Autoresonant Excitation of Antiproton Plasmas, Phys. Rev. Lett. **106**, 025002 (2011).

[80] J. R. Danielson, T. R. Weber, and C. M. Surko, Plasma Manipulation Techniques for Positron Storage, Phys. Plasmas **13**, 123502 (2006).

[81] N. C. Hurst, J. R. Danielson, C. J. Baker, and C. M. Surko, Confinement and Manipulation of Electron Plasmas in a Multicell Trap, Phys. Plasmas **26**, 013513 (2019).

[82] M. Ahmadi, et al., Antihydrogen Accumulation for Fundamental Symmetry Tests, Nature Communications **8**, 681 (2017).

[83] L. V. Jorgensen, et al., New Source of Dense, Cryogenic Positron Plasmas, Phys. Rev. Lett. **95**, 025002 (2005).

[84] D. W. Fitzakerley, et al., Electron Cooling and Accumulation of 4 x 10^9 Positrons in a System for Longterm Storage of Antihydrogen Atoms, Bull. Am. Phys. Soc. **58**, 176 (2013).

[85] M. R. Natisin, J. R. Danielson, and C. M. Surko, Formation Mechanisms and Optimization of Trap-Based Beams, Phys. Plasmas **23**, 023505 (2016).

[86] D. B. Cassidy, et al., Experiments with a High-Density Positronium Gas, Phys. Rev. Lett. **95**, 195006 (2005).

[87] D. B. Cassidy, S. H. M. Deng, H. K. M. Tanaka, and A. P. Mills, Single Shot Positron Annihilation Lifetime Spectroscopy, Appl. Phys. Lett. **88**, 194105 (2006).

[88] M. Maekawa and A. Kawasuso, Development of Pulsed Positron Beam Line with Compact Pulsing System, Nucl. Instrum. Meth. B **270**, 23 (2012).

[89] R. G. Greaves and C. M. Surko, Positron Trapping and the Creation of High-Quality Trap-Based Positron Beams, Nucl. Instrum. Methods B **192**, 90 (2002).

[90] W. Stoeffl, P. Asoka-Kumar, and R. Howell, The Positron Microprobe at Lawrence Livermore National Laboratory, Appl. Surf. Sci. **149**, 1 (1999).

[91] A. P. Mills, Brightness Enhancement of Slow Positron Beams, Appl. Phys. **23**, 189 (1980).

[92] D. B. Cassidy, S. H. M. Deng, R. G. Greaves, and A. P. Mills, Accumulator for the Production of Intense Positron Pulses, Rev. Sci. Instrum. **77**, 073106 (2006).

[93] D. B. Cassidy, V. E. Meligne, and A. P. Mills, Production of a Fully Spin-Polarized Ensemble of Positronium Atoms, Phys. Rev. Lett. **104**, 173401 (2010).

[94] M. Charlton and J. W. Humberston, *Positron Physics* (Cambridge Univ. Press, Cambridge, U. K., 2001).

[95] D. B. Cassidy, T. H. Hisakado, H. W. K. Tom, and A. P. Mills, Efficient Production of Rydberg Positronium, Phys. Rev. Lett. **108**, 043401 (2012).

[96] M. Charlton, Antihydrogen Production in Collisions of Antiprotons with Excited States of Positronium, Physics Letters A **143**, 143 (1990).

[97] C. H. Storry, et al., First Laser-Controlled Antihydrogen Production, Phys. Rev. Lett. **93**, 263401 (2004).

[98] K. Michishio, L. Chiari, F. Tanaka, N. Oshima, and Nagashima, A High-Quality and Energy-Tunable Positronium Beam System Employing a Trap-Based Positron Beam, Rev. Sci. Instrum. **90**, 023305 (2019).

[99] P. F. Barker and M. Charlton, Directed Fluxes of Positronium Using Pulsed Travelling Optical Lattices, New J. Phys. 045005 (2012).

[100] M. Amoretti, et al., Production and Detection of Cold Antihydrogen Atoms, Nature **419**, 456 (2002).

[101] G. Gabrielse, et al., Driven Production of Cold Antihydrogen and the First Measured Distribution of Antihydrogen States, Phys. Rev. Lett. **89**, 233401 (2002).

[102] G. B. Andresen, et al., Confinement of Antihydrogen for 1,000 Seconds, Nature Physics **7**, 558 (2011).

[103] J. S. Hangst, in *Spectroscopic and gravitational measurements on antihydrogen: ALPHA-3, ALPHA-g and beyond*, CERN-SPSC-2019-036 ; SPSC-P-362 (CERN, Geneva Switzerland, 2019).

[104] M. Ahmadi, et al., Observation of the 1S-2P Lyman-Alpha Transition in Antihydrogen, Nature **561**, 211 (2018).

[105] A. C. L. Jones, et al., Focusing of a Rydberg Positronium Beam with an Ellipsoidal Electrostatic Mirror, Phys. Rev. Lett. **119**, 053201 (2017).

[106] C. Amole, et al., In Situ Electromagnetic Field Diagnostics with an Electron Plasma in a Penning–Malmberg Trap, New J. Phys. **16**, 013037 (2014).

[107] M. Affolter, F. Anderegg, and C. F. Driscoll, Space Charge Frequency Shifts of the Cyclotron Modes in Multi-Species Ion Plasmas, J. Am. Soc. Mass Spectrom. **26**, 330 (2015).

[108] E. D. Hunter, et al., Electron Cyclotron Resonance (Ecr) Magnetometry with a Plasma Reservoir, arXiv:1912.04358 (2019).

[109] J. R. Danielson, T. R. Weber, and C. M. Surko, Extraction of Small-Diameter Beams from Single-Component Plasmas, Appl. Phys. Lett. **90**, 081503 (2007).

[110] A. Passner, C. M. Surko, M. Leventhal, and A. P. Mills, Ion Production by Positron-Molecule Resonances, Phys. Rev. A **39**, 3706 (1989).

[111] L. D. Hulett, J. Xu, S. A. McLuckey, T. A. Lewis, and D. M. Schrader, The Ionization of Organic Molecules by Slow Positrons, Can. J. Phys. **74**, 411 (1996).

[112] L. D. Hulett, J. Xu, S. A. ÂcLuckey, and D. M. Schrader, The Interaction of Slow Positrons with Organic Molecules above and Below Positronium Formation Thresholds, J. of Radioanal. and Nucl. Chem. **210**, 309 (1996).

[113] F. A. Gianturco and R. R. Lucchese, Computational Investigation of Positron Scattering from C_{60}, Phys. Rev. A **60**, 4567 (1999).

[114] C. Hugenschmidt, Positrons in Surface Physics, Surf. Sci. Reports **71**, 547 (2016).

[115] G. Laricchia and H. R. J. Walters, Positronium Collision Physics, Rivista del Nuovo Cimento **35**, 305 (2012).

[116] I. I. Fabrikant, G. F. Gribakin, and R. S. Wilde, Positronium Collisions with Atoms and Molecules, Journal of Physics Conferece Series **875**, 012001 (2017).

[117] C. Hugenschmidt, Present and Future Experiments Using Bright Low-Energy Positron Beams, J. Phys. B: Conf. Series **791**, 012002 (2017).

[118] D. Chaudhary, M. R. Went, K. Nakagawa, S. Buckman, and J. P. Sullivan, Molecular Pore Size Characterization within Chitosan Biopolymer Using Positron Annihilation Lifetime Spectroscopy, Mater. Lett. **64**, 2635 (2010).

[119] A. C. L. Jones, et al., Monoenergetic Positronium Emission from Metal-Organic Framework Crystals, Phys. Rev. Lett. **114**, 153201 (2015).

[120] K. F. Canter, Low Energy Positron and Positronium Diffraction., in *Positron Scattering in Gases*, edited by J. W. Humberston and M. R. C. McDowell (Plenum, New York, 1983), p. 219.

[121] A. P. Mills, New Experiments with Bright Positron and Positronium Beams, in *New Directions in Antimater Chemistry and Physics*, edited by C. M. Surko and F. A. Gianturco (Kluwer Academic, Netherlands, 2001), p. 115.

[122] A. P. Mills, Positronium Molecule Formation, Bose-Einstein Condensation and Stimulated Annihilation, Nucl. Instrum. Methods B **192**, 107 (2002).

[123] V. Tsytovich and C. B. Wharton, Laboratory Electron-Positron Plasma-a New Research Object, Comments Plasma Phys. Controlled Fusion **4**, 91 (1978).

[124] T. S. Pedersen, et al., Plans for the Creation and Studies of Electron–Positron Plasmas in a Stellarator, New J. Phys. **14**, 035010 (2012).

[125] C. M. Surko, J. R. Danielson, and T. R. Weber, Accumulation, Storage and Manipulation of Large Numbers of Positrons in Traps {Ii}. – Selected Topics, in *Physics with Many Positrons*, edited by A. P. Mills and A. Dupasquier (IOS press, Amsterdam, 2010), p. 545.

[126] E. V. Stenson, et al., Lossless Positron Injection into a Magnetic Dipole Trap, Phys. Rev. Lett. **121**, 235005 (2018).

[127] J. Horn-Stanja, et al., Confinement of Positrons Exceeding 1 Second in a Supported Magnetic Dipole Trap, Phys. Rev. Lett. **121**, 235003 (2018).

[128] H. Yabu, Many Positron and Positronium Interactions, Nuc. Instrum. Meth. B **221**, 144 (2004).

[129] E. M. Bass and D. H. E. Dubin, Antihydrogen Formation from Antiprotons in a Pure Positron Plasma, Phys. Plasmas **16**, 012101 (2008).

[130] F. Robicheaux and J. D. Hanson, Three-Body Recombination for Protons Moving in a Strong Magnetic Field, Phys. Rev. A **69**, 010701 (R) (2004).

[131] F. Robicheaux, Simulations of Antihydrogen Formation, Phys. Rev. A **70**, 022510 (2004).

[132] S. Jonsell and M. Charlton, Formation of Antihydrogen Beams from Positron–Antiproton Interactions, New J. Phys. **21**, 073020 (2019).

[133] W. Grabowski, Gbar - Principle of the Experiment. https://gbar.web.cern.ch/GBAR/public/en/principle.html

[134] Y. Enomoto, et al., Synthesis of Cold Antihydrogen in a Cusp Trap, Phys. Rev. Lett. **105**, 243401 (2010).

[135] A. Kellerbauer, et al., Proposed Antimatter Gravity Measurement with an Antihydrogen Beam, Nucl. Instrum. Meth. B **266**, 351 (2008).

[136] J. Adam, et al., Beam Energy Dependence of (Anti-)Deuteron Production in Au + Au Collisions at the Bnl Relativistic Heavy Ion Collider, Phys. Rev. C **99**, 064905 (2019).

[137] A. I. Zhmoginov, A. E. Charman, R. Shalloo, J. Fajans, and J. S. Wurtele, Nonlinear Dynamics of Anti-Hydrogen in Magnetostatic

Traps: Implications for Gravitational Measurements, Class. Quantum Grav. **30**, 205014 (2013).
[138] C. Hugenschmidt, C. Piochacz, M. Reiner, and K. Schreckenbach, The Nepomuc Upgrade and Advanced Positron Beam Experiments, New J. Phys. **14**, 055027 (2012).
[139] ELENA doi: 10.1098/rsta.2017.0266
[140] Physicists Plan Antimatter's First Outing — in a Van, Nature **554**, 412 (2018).
[141] S. Ulmer, et al., 2019), https://cds.cern.ch/record/002702758.